Am J Physiol Endocrinol Metab 304: E495–E506, 2013.
First published December 31, 2012; doi:10.1152/ajpendo.00518.2012.

Skeletal muscle uncoupling-induced longevity in mice is linked to increased substrate metabolism and induction of the endogenous antioxidant defense system

S. Keipert,[1] M. Ost,[1] A. Chadt,[1,2] A. Voigt,[1] V. Ayala,[3] M. Portero-Otin,[3] R. Pamplona,[3] H. Al-Hasani,[1,2] and S. Klaus[1]

[1]*German Institute of Human Nutrition, Potsdam-Rehbruecke, Germany;* [2]*German Diabetes Center, Düsseldorf, Germany; and* [3]*Department of Experimental Medicine, University of Lleida-Biomedical Research Institute of Lleida, Lleida, Spain*

Submitted 18 October 2012; accepted in final form 28 December 2012

Keipert S, Ost M, Chadt A, Voigt A, Ayala V, Portero-Otin M, Pamplona R, Al-Hasani H, Klaus S. Skeletal muscle uncoupling-induced longevity in mice is linked to increased substrate metabolism and induction of the endogenous antioxidant defense system. *Am J Physiol Endocrinol Metab* 304: E495–E506, 2013. First published December 31, 2012; doi:10.1152/ajpendo.00518.2012.—Ectopic expression of uncoupling protein 1 (UCP1) in skeletal muscle (SM) mitochondria increases lifespan considerably in high-fat diet-fed UCP1 Tg mice compared with wild types (WT). To clarify the underlying mechanisms, we investigated substrate metabolism as well as oxidative stress damage and antioxidant defense in SM of low-fat- and high-fat-fed mice. Tg mice showed an increased protein expression of phosphorylated AMP-activated protein kinase, markers of lipid turnover (p-ACC, FAT/CD36), and an increased SM ex vivo fatty acid oxidation. Surprisingly, UCP1 Tg mice showed elevated lipid peroxidative protein modifications with no changes in glycoxidation or direct protein oxidation. This was paralleled by an induction of catalase and superoxide dismutase activity, an increased redox signaling (MAPK signaling pathway), and increased expression of stress-protective heat shock protein 25. We conclude that increased skeletal muscle mitochondrial uncoupling in vivo does not reduce the oxidative stress status in the muscle cell. Moreover, it increases lipid metabolism and reactive lipid-derived carbonyls. This stress induction in turn increases the endogenous antioxidant defense system and redox signaling. Altogether, our data argue for an adaptive role of reactive species as essential signaling molecules for health and longevity.

uncoupling protein 1; AMP-activated protein kinase; oxidative stress; redox signaling; lipid metabolism

AGING IS A VERY COMPLEX PROCESS driven by numerous molecular pathways and biochemical events. Regarding the relationship between energy metabolism and longevity, there is a hypothesis termed "uncoupling to survive," which suggests that increased mitochondrial uncoupling and thus increased energy expenditure might increase longevity by preventing the formation of reactive oxygen species (ROS) (6). Previously, we showed that transgenic (Tg) mice with an ectopic expression of the uncoupling protein 1 (UCP1) in skeletal muscle (UCP1 Tg mice) showed a delayed development of obesity, improved glucose tolerance, and a 42% increased median lifespan compared with their wild-type (WT) littermates when exposed to a high-fat diet (30). However, the molecular mechanisms for these beneficial health effects of skeletal muscle uncoupling are not yet clarified.

Address for reprint requests and other correspondence: S. Klaus, German Institute of Human Nutrition, Arthur Scheunert Allee 114-116, 14558 Nuthetal, Potsdam-Rehbruecke, Germany (e-mail: klaus@dife.de).

One hallmark of UCP1 Tg mice is an increased insulin sensitivity independent of body weight. Insulin resistance plays a crucial part in the pathogenesis of the metabolic syndrome and is characterized by a reduced substrate metabolism and impaired defense against stress in skeletal muscle. Skeletal muscle (SM) uncoupling increases SM glucose uptake and activates the AMP-activated protein kinase (AMPK) (17, 38). AMPK, a master regulator of cellular energy homeostasis, is involved in several ways in the aging process (reviewed in Ref. 52). For example, AMPK increases mitochondrial biogenesis, regulates the activity of the histone/protein deacetylase sirtuin 1 (SIRT1) (8), and inhibits the activity of mammalian target of rapamycin (mTOR) (57), which are postulated to regulate lifespan (49, 55). Thus, AMPK could be a key regulator in our UCP1 Tg mouse model for enhancing insulin sensitivity and lifespan. On the other hand, it is conceivable that mild uncoupling through UCPs affects cellular mitochondrial ROS production and thus might impact aging. We could show a decreased ROS production in isolated mitochondria in UCP1 Tg mice (29). However, so far it is not known whether or how UCP1, which leads to an increased metabolic rate, regulates superoxide production in the body. Furthermore, it is quite intensively discussed which role oxidative stress and the accumulation of cellular damage play in the aging process (41, 53). Central to oxidative stress is the generation of reactive species, including ROS and reactive carbonyl species, which are derived from the interaction of ROS with lipids and carbohydrates and lead to an increase in oxidatively modified damaged proteins, carbohydrates, lipids, and DNA. Furthermore, the accumulation of ROS-induced damage is linked to several age-related pathologies, including type 2 diabetes, which is associated with muscle insulin resistance (15, 25). Specifically, obesity-induced insulin resistance is characterized by increased oxidative stress, inflammation, and impaired defense against stress (60). But the toxicity of ROS is only one aspect of its action in living cells. They can also modulate the function of several signaling pathways, such as stress response pathways [heat shock proteins (HSPs), MAPK] or antioxidant response systems, and thereby stimulate beneficial adaption to cellular stresses. This is in line with the mitochondrial hormesis hypothesis, suggesting that ROS are essential signaling molecules for health and longevity (47). Thus, it depends strongly on the magnitude of oxidative stress, duration of exposure, and the target organ if reactive species induce oxidative damage on the one hand or acts as an important signaling molecule on the other hand.

The mechanisms that determine an organism's lifespan are complex and poorly understood, and the roles of AMPK or reactive species in the aging process are discussed controversially. Nevertheless, an effective energy metabolic homeostasis

as well as enhanced stress resistance are the hallmarks of improved and extended lifespan.

In this study, we investigate the skeletal muscle mitochondrial uncoupling-induced longevity effect in UCP1 Tg mice. The aim was to clarify the molecular mechanisms in skeletal muscle that are responsible for the "healthy" phenotype of young UCP1 Tg mice on a high-fat diet and whether it is a consequence of oxidative stress or improved substrate metabolism.

METHODS

Animal maintenance. UCP1 Tg animals were generated as described previously (32). Experiments were performed with male UCP1 Tg and WT controls maintained on a mixed C57BL/6-CBA background. Mice were housed in groups with ad libitum access to food and water. At 12 wk of age, mice were switched from standard chow diet to two different semisynthetic diets, a low-fat diet and a high-fat diet (diet composition; see Ref. 28). In the first week of dietary switch, food intake was measured (TSE Systems). At 20 wk of age (8 wk on diet), mice were euthanized in the morning 2 h after food withdrawal, and plasma and tissue samples were collected. This time point was chosen because previous results showed that UCP1 Tg mice are protected against diet-induced obesity within the first 10 wk of dietary intervention, whereas in older age they become obese like WT littermates (30). We support the view that this delayed development of obesity is crucial for the effect on longevity, and effects could possibly be masked at a later time point when these mice start to develop obesity.

With a subgroup of high-fat diet-fed mice, ex vivo fatty acid oxidation in muscle was measured. Animal maintenance and experiments were approved by the animal welfare committee of the Ministry of Agriculture and Environment (State of Brandenburg, Germany).

Immunological detection. Protein was extracted from skeletal muscle (quadriceps and gastrocnemius), as described previously (39). Sodium dodecyl sulfate polyacrylamide gel electrophoresis and incubation of different antibodies, as well as chemiluminescence detection and quantification of protein bands, were done as described before (39). The following primary antibodies were used: UCP1 and UCP3 (Abcam), p-AMPK Thr^{172}, AMPK, p-ACC Ser^{79}, ACC, porin, p-mTOR Ser^{2448}, mTOR, p-S6P $Ser^{235/236}$, p-4E-BP $Thr^{37/46}$, 4E-BP, p-ERK1/2 $Thr^{202/}Tyr^{204}$, ERK1/2, p-SAPK/JNK1/2 $Thr^{183/}Tyr^{185}$, SAPK/JNK1/2 (Cell Signaling Technology), oxidative phosphorylation complexes (Acris), CD36 (R & D Systems), HSP25 and HSP70 (Stressgen), and α-tubulin (Sigma-Aldrich). The following horseradish peroxidase-conjugated secondary antibodies were used: anti-rat (R & D Systems), anti-rabbit IgG, or anti-mouse IgG (Cell Signaling Technology).

Analyses of fatty acid oxidation. Assays were done essentially as described (2, 9). Mice were fasted for 4 h prior to the study. Then extensor digitorum longus (EDL) and soleus muscles were removed from anesthetized mice (99% 2,2,2-tribromo ethanol and tertiary amyl alcohol at 20 μl/g body wt ip; Avertin) and incubated for 15 min at 30°C in vials containing preoxygenated (95% O_2-5% CO_2) Krebs-Henseleit buffer supplemented with 15 mM mannitol, 5 mM glucose, and 3.5% fatty acid-free BSA. Subsequently, muscles were transferred to new vials containing freshly pregassed Krebs-Henseleit buffer with 4 mCi/ml [^{3}H]palmitate and 300 mM unlabeled palmitate at 30°C for 2 h. One EDL and one soleus muscle per mouse were stimulated with 2 mM AICAR (5-aminoimidazole-4-carboxamide 1-β-D-ribofuranoside, 2 mM; Biomol International) during this incubation step. After absorption of fatty acids to activated charcoal, fatty acid oxidation was determined by measuring tritiated water using a scintillation counter.

Quantitative RT-PCR. RNA was isolated from tissue as described before (10), with modifications as described by Weber et al. (61). Synthesis of cDNA was performed from 1 μg of total RNA using the RevertAid H Minus First Strand cDNA Synthesis Kit (Fermentas). Quantitative real-time PCR was performed on the Applied Biosystems 7900 HT Fast Real-Time PCR System (Applied Biosystems). The PCR mix (5 μl) contained TaqMan or SYBR Green Universal PCR Master Mix (Applied Biosystems) and a cDNA amount corresponding to 5 ng of RNA used for cDNA synthesis and gene-specific primer-probe pairs (Sirt1: forward cagaccctcaagccatgttt, reverse gatcct-tgggattcctgcaa;PGC1α: forward ctacagacaccgcac acacc, reverse gcgctcttcaattgctttct, probe 6-FAM-cccgcttctcgtgctctttgc-TAMRA). Gene expression was calculated as ΔC_T, using β-actin (forward tgttac-caactgggacgaca, reverse ggggtgttgaaggtctcaaa, probe 6-FAM-accgt-gaaaagatgacccag-TAMRA) as a reference, and expressed relative to the WT group normalized to a value of one.

Triglyceride analysis. The triglyceride concentrations of liver and skeletal muscle were measured after extraction with 10 mmol/l sodium phosphate buffer (pH 7.4) containing 1 mmol/l EDTA and 1% polyoxyethylene (10) tridecyl ether using the Triglyceride Determination Kit (Sigma-Aldrich).

Catalase activity. A catalase (CAT) activity assay kit (Cayman Europe) was used to determine the activity level of CAT in muscles and plasma according to the manufacturer's recommendations. Thirty grams of muscle tissue was immersed in a 450-μl buffer containing 50 mM Kaliumphosphat and 1 mM EDTA (pH 7.0), homogenized for 2 min in Speed Mill P12, and centrifuged at 10,000 *g* for 30 min at 4°C. The supernatant was used to determine the protein content (see above) and CAT activity levels in muscle. After the appropriate incubations, the samples were read at an absorbance of 520 nm using a 96-well plate reader. Muscle samples were normalized to protein content.

Superoxide dismutase activity. The commercially available Superoxide Dismutase (SOD) Assay Kit II (Cayman Europe) was used to measure total SOD activity. Muscle tissue was homogenized in a buffer (20 mM HEPES, 1 mM EGTA, 210 mM mannitol, and 70 mM sucrose, pH 7.2, for 2 min in Speed Mill P12) and centrifuged at 1,500 *g* for 10 min at 4°C. The supernatant was used to determine the protein content and SOD activity levels in muscle. The absorbance was measured at 450 nm using a 96-well plate reader. Muscle samples were normalized to protein content.

Aconitase activity. Aconitase activity was determined spectrometrically as described previously (51) by monitoring the formation of NADPH at 340 nm. The assay mixture contained 50 mM Tris·HCl, pH 7.4, 60 mM sodium citrate, 1 mM $MnCl_2$, 0.4 mM $NADP^+$, and 4 U $NADP^+$ isocitrate dehydrogenase for a final volume of 1 ml. Tissue (muscle/liver) was homogenized in homogenization buffer (50 mM Tris, pH 7.4, for 3 min in Speed Mill P12) and centrifuged at 23,000 *g* for 5 min at 4°C. The supernatant was used to determine the protein content and aconitase activity levels in the tissues. An appropriate volume tissue extract (30 μg protein) was brought up to 150 μl with 50 mM Tris·HCl and loaded into one well of a 96-well plate. To start the reaction, 150 μl of assay mixture was added, and the absorbance change at 340 nm was measured for 60 min at 37°C. The aconitase activity was calculated from the slope of the linear portion.

Oxidative damage markers. Ne-(malondialdehyde)lysine (MDA), Ne-(carboxymethyl)lysine (CML), Ne-(carboxyethyl)lysine (CEL), glutamic semialdehyde (GSA), and aminoadipic semialdehyde (AASA) were determined as trifluoroacetic acid methyl ester derivatives in acid-hydrolyzed delipidated and reduced protein samples by GC-MS using a HP6890 Series II gas chromatograph (Agilent, Barcelona, Spain) with a MSD5973A Series and a 7683 Series automatic injector, a HP-5MS column (30 m × 0.25 mm × 0.25 μm) and the described temperature program (42). Quantification was performed by internal and external standardization using standard curves constructed from mixtures of deuterated and nondeuterated standards. Analyses were carried out by selected ion-monitoring GC-MS. The ions used were lysine and [$^2H_8$]lysine, *m/z* 180 and 187, respectively; 5-hydroxy-2-aminovaleric acid and [$^2H_5$]5-hydroxy-2-aminovaleric acid (stable derivatives of GSA), *m/z* 280 and 285, respectively; 6-hydroxy-2-aminocaproic acid and [$^2H_4$]6-hydroxy-2-aminocaproic acid (stable derivatives of AASA), *m/z* 294 and 298, respectively; CML and [$^2H_4$]CML, *m/z* 392 and 396,

Table 1. *Phenotypic data of WT and UCP1 Tg mice fed a high-fat or a low-fat diet for 8 wk*

Biometrical Data	Low Fat		High Fat		ANOVA	
	WT	UCP1 Tg	WT	UCP1 Tg	Diet	Genotype
Body weight, g	31.7 ± 0.7	20.3 ± 0.3***	39.2 ± 1.3	22.2 ± 1.0***	<0.0001	<0.0001
Lean body mass, g	26.6 ± 0.7	17.6 ± 0.3***	25.0 ± 0.8	18.3 ± 0.8***	NS	<0.0001
Body fat mass, g	6.4 ± 0.9	3.0 ± 0.1***	14.2 ± 1.0	3.9 ± 0.4***	<0.0001	<0.0001
Body fat mass, %body mass	20.2 ± 2.7	14.7 ± 0.6*	36.6 ± 2.1	17.8 ± 1.2***	<0.0001	<0.0001
Body length, cm	10.6 ± 0.1	10.0 ± 0.1**	10.8 ± 0.1	10.1 ± 0.1**	NS	<0.0001
Food intake, kJ·5 days^{-1}·g body mass^{-1}	13.9 ± 0.8	16.5 ± 1.2	15.3 ± 1.0	23.7 ± 1.9**	<0.05	<0.0001
Cum Food intake, kJ/5 days†	358 ± 23	295 ± 30	412 ± 17	398 ± 30	<0.05	NS
Insulin, μg/l	0.89 ± 0.14	0.82 ± 0.28	4.12 ± 1.22	0.92 ± 0.24***	<0.001	<0.001
Blood glucose, mmol/l	6.49 ± 0.35	6.08 ± 0.32	7.48 ± 0.51	6.68 ± 0.60	NS	NS
Muscle quadriceps, g	0.43 ± 0.01	0.18 ± 0.02***	0.43 ± 0.01	0.17 ± 0.02***	NS	<0.0001
Muscle quadriceps, g/100 g lean body mass	1.61 ± 0.03	1.04 ± 0.01***	1.73 ± 0.06	0.95 ± 0.12***	NS	<0.0001
Muscle triglyceride, mg/mg protein	0.64 ± 0.12	0.48 ± 0.11	0.83 ± 0.19	0.41 ± 0.07	NS	<0.05
Liver weight, g	1.34 + 0.05	0.92 + 0.03***	1.42 + 0.07	0.93 + 0.03***	NS	<0.0001
Liver weight, g/100 g lean body mass	5.07 ± 0.24	5.22 ± 0.17	5.72 ± 0.34	5.13 ± 0.22	NS	NS
Liver triglyceride, mg/mg protein	0.41 ± 0.04	0.30 ± 0.03*	0.87 ± 0.12	0.36 ± 0.04***	<0.001	<0.0001

Data are shown as means ± SE; n = 8–10. WT, wild type; UCP1, uncoupling protein 1; Tg, transgenic; NS, not significant. *$P < 0.05$, **$P < 0.01$, and ***$P < 0.0001$, significant differences between the genotypes within 1 diet group. †First 5 days after dietary switch.

respectively; CEL and [$^2H_4$]CEL, *m/z* 379 and 383, respectively; and MDAL and [$^2H_8$]MDAL, *m/z* 474 and 482, respectively. The amounts of product were expressed as micromoles of GSA, AASA, CML, CEL, or MDAL per mole of lysine.

Statistics. Statistical analyses were performed using Stat Graph Prism (5.0). Data are reported as means ± SE. One-way or two-way ANOVA was used to evaluate differences between groups with appropriate post hoc tests. Statistical significance was assumed at $P < 0.05$.

RESULTS

Body composition, insulin sensitivity, and tissue triglyceride levels. WT animals on the high-fat diet showed increased body fat compared with the low-fat diet, whereas UCP1 Tg mice showed no dietary differences in body weight or body fat. Independent of the diet, UCP1 Tg mice were much lighter (reduced lean mass and size) but also leaner (reduced body fat content), and they showed no differences in blood glucose but lower insulin levels on a high-fat diet, indicating a higher insulin sensitivity compared with WT (Table 1). Interestingly, energy intake was not significantly different between the genotypes. Moreover, relative to body weight, UCP1 Tg mice had a higher food intake compared with WT mice on both diets. WT and UCP1 Tg mice showed the same weight-specific liver weight, but UCP1 Tg mice displayed a strong decrease in muscle mass (Table 1). WT mice on a high-fat diet showed significantly increased liver triglycerides and a tendency toward higher muscle triglycerides compared with the other three groups (Table 1).

Expression of uncoupling proteins in muscle. We analyzed UCP1 and -3 protein expression by Western blot. As shown in Fig. 1*A*, UCP1 was detectable only in skeletal muscle from UCP1 Tg mice, with no additional influence of the diet. To examine whether the transgenic expression of UCP1 influences UCP3, the main uncoupling protein expressed in the skeletal muscle, we determined the amount of UCP3 protein by Western blot. As seen in Fig. 1, *A* and *B*, there was no difference between the genotypes on a low-fat diet. However, exposing WT mice to a high-fat diet resulted in increased UCP3 protein expression.

Substrate metabolism and mitochondrial biogenesis in skeletal muscle. To investigate whether skeletal muscle uncoupling leads to an energy demand in the muscle cell, we looked at AMPK, a protein that acts as an energy sensor and regulates substrate metabolism in the cell. In UCP1 Tg animals, AMPK phosphorylation in skeletal muscle was increased significantly compared with WT (Fig. 2, *A* and *B*), indicating an increased

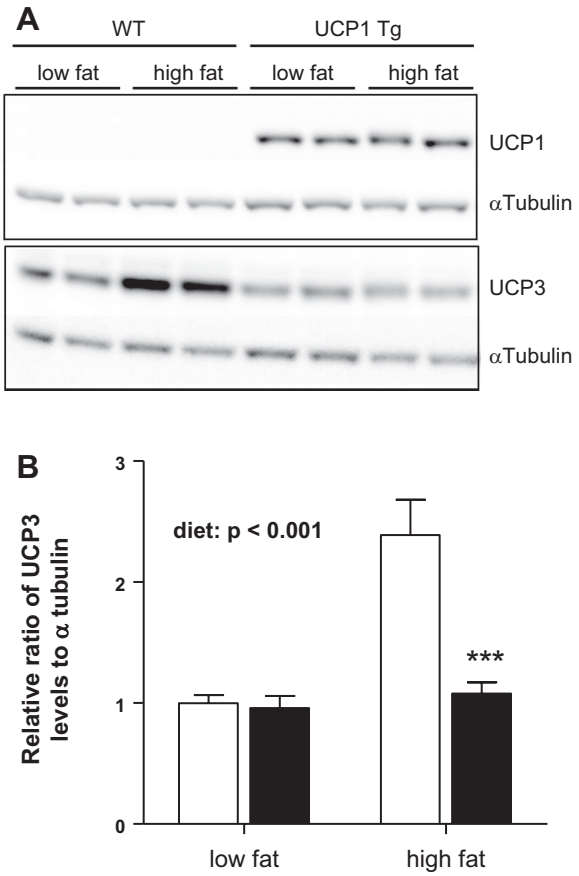

Fig. 1. Uncoupling protein (UCP) expression in skeletal muscle. *A*: Western blot analyses of skeletal muscle protein levels of UCP1 and -3. *B*: relative ratio of UCP3 to α-tubulin of wild-type (WT; open bars) and UCP1 transgenic (Tg) mice (filled bars) fed a low-fat or high-fat diet. ***$P < 0.0001$, significant differences between the genotypes within 1 diet group (data are shown as means ± SE relative to the WT low-fat group; n = 7).

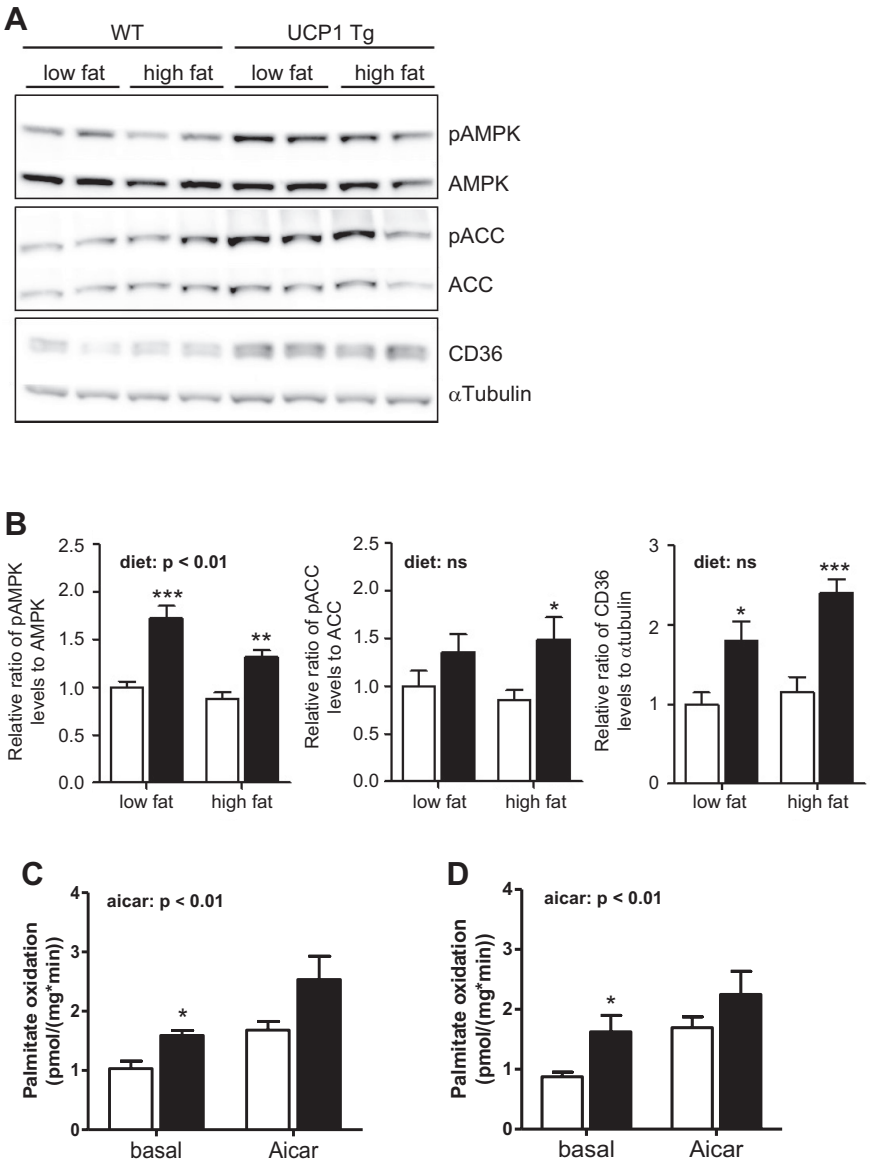

Fig. 2. Fatty acid metabolism in skeletal muscle. *A*: Western blot analyses of skeletal muscle protein levels. *B*: relative ratio of p-AMPK to AMPK, p-ACC to ACC, and CD36 to α-tubulin of WT (open bars) and UCP1 Tg mice (filled bars) fed a low-fat or high-fat diet (data are shown as means ± SE relative to the WT low-fat group). Ex vivo fatty acid oxidation in isolated soleus (more oxidative; *C*) and extensor digitorum longus muscle (more glycolytic; *D*) of WT and UCP1 Tg mice fed a high-fat diet. $*P < 0.05$, $**P < 0.001$, and $***P < 0.0001$, significant differences between the genotypes within 1 diet/treatment group (data are shown as means ± SE; $n = 7$). NS, not significant.

AMPK activity. To analyze fatty acid oxidation in detail, we measured ACC, fatty acid transporter CD36 (Fig. 2, *A* and *B*), and (on the high-fat diet only) directly ex vivo fatty acid oxidation in isolated soleus muscle (mostly oxidative fibers; Fig. 2*C*) and EDL muscle (mostly glycolytic fibers; Fig. 2*D*). UCP1 Tg animals had a significantly increased protein phosphorylation of ACC, a direct downstream factor of AMPK. Also, CD36 protein expression was increased in skeletal muscle (Fig. 2, *A* and *B*). In UCP1 Tg animals, ex vivo basal fatty acid oxidation was increased significantly in both muscle types but more pronounced in the glycolytic EDL (EDL +85%, $P = 0.0038$; soleus +54%, $P = 0.038$ compared with WT; Fig. 2, *C* and *D*). When AICAR, a known AMPK activator, was added, WT mice showed a significant increase in palmitate oxidation in both muscle types, whereas this effect was less in isolated muscles from UCP1 Tg animals.

It is known that AMPK increases mitochondrial biogenesis. On gene expression level we found a slight, nonsignificant increase in PGC-1α and a significant increase in SIRT1 in SM of UCP1 TG mice (Fig. 3, *A* and *B*). Protein levels of most of the oxidative phosphorylation complexes and porin, both of which are markers for mitochondrial content, were similar in skeletal muscle homogenates of WT and UCP1 Tg mice independent of the diet (Fig. 4, *A* and *B*). These data are compatible with a lack of structural changes in SM mitochondria induced by UCP1 (data not shown).

AMPK is a well-known inhibitor of mTOR; therefore, we investigated mTOR as well as several downstream factors. We could not detect any differences in mTOR or phosphorylated mTOR protein expression between the genotypes (Fig. 5A). The downstream mTOR target S6 protein phosphorylation (Fig. 5*A*) was also not affected. Total as well as phosphorylated 4E-BP, which is also a downstream target of mTOR, was strongly increased in UCP1 Tg animals compared with WT (Fig. 5*A*).

Oxidative stress status in SM. To analyze the oxidative stress status in muscle, we measured oxidatively induced protein damage, antioxidant capacity, and ROS-induced signaling pathways in skeletal muscle. Five markers of oxidative protein

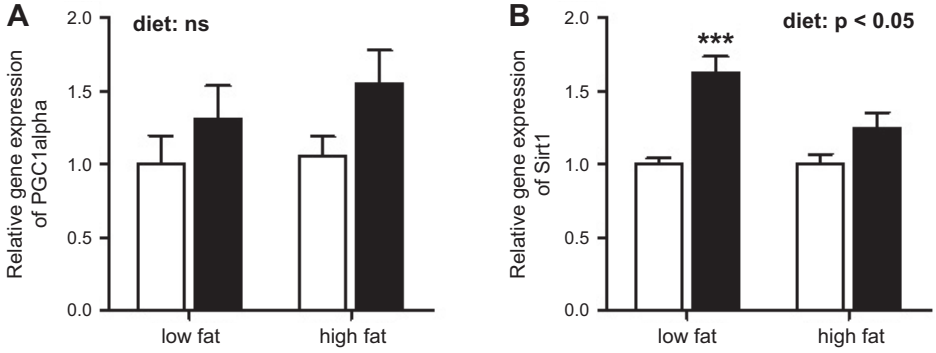

Fig. 3. Gene expression of PPARγ coactivator-1α (PGC-1α; *A*) and sirtuin 1 (Sirt1; *B*) in skeletal muscle of WT (open bars) and UCP1 Tg mice (filled bars) fed a low-fat or high-fat diet. ***$P <$ 0.0001, significant differences between the genotypes within 1 diet (data are shown as means ± SE relative to the WT low-fat group; $n = 7$).

damage were measured by mass spectrometry in skeletal muscle and liver protein from WT and UCP1 Tg mice. We used markers of direct oxidation of proteins (GSA, AASA) and of carbonyl-amine reactions such as lipoxidation and glycoxidation (CML, MDA, CEL) (Table 2) (23, 42). Levels of MDA, which are derived from protein adducts of lipid peroxidation products, were increased significantly in skeletal muscle of UCP1 Tg mice on both diets compared with WT. Moreover, AASA, a carbonyl product of metal-catalyzed protein oxidation, was increased in UCP1 Tg mice on a low-fat diet. CML, CEL, and GSA were not influenced by the genotype. In contrast to skeletal muscle, UCP1 Tg mice showed decreased MDA levels in the liver compared with WT mice.

Regarding the endogenous antioxidant defense system, UCP1 Tg animals showed significantly increased antioxidative enzyme activities in SM compared with WT. CAT activity was increased in both diets (Fig. 6*A*), whereas SOD activity was increased only on the high-fat diet (Fig. 6*B*). In plasma, there were no genotype differences in these two antioxidant enzymes (data not shown). Interestingly, aconitase activity, which is a sensitive target for free radicals and postulated to be a marker for oxidative stress, was increased in muscle but not in liver (Table 2) of UCP1 TG animals.

Another important role in cellular stress response is played by the family of HSPs. In skeletal muscle of UCP1 Tg mice, the expression of HSP25 was significantly upregulated in both diets, whereas there were no differences in HSP70 (Fig. 7). The increased stress response and the higher lipoxidative molecular damage might suggest an increased oxidative stress status in UCP1 Tg mice. Lipid-derived carbonyls have been linked to the activation of redox-sensitive signaling pathways such as the MAPKs. In skeletal muscle, several signaling proteins of the MAPK family are expressed, and we analyzed four of them: ERK1 and -2 and c-Jun NH_2-terminal kinases (JNK) 1 and 2. The phosphorylation ratio of p-ERK1/ERK1 and p-JNK2/JNK2 was not affected by genotype or diet (Fig. 8). The pERK2/ERK2 and pJNK1/JNK1 ratios were upregulated significantly in UCP1 Tg mice (Fig. 8*B*), indicating an increased activity of these kinases. The only diet-dependent effect was an increased p-JNK1/JNK1 ration in WT high-fat diet-fed mice.

DISCUSSION

We have reported previously that skeletal muscle mitochondrial uncoupling alleviates the detrimental effects of high-fat diets on metabolic status and longevity (30). In this study, we focused on the molecular mechanisms triggered by UCP1 ectopically expressed in mouse skeletal muscle. The current study demonstrates that skeletal muscle uncoupling led to an energy demand in the muscle tissue that was reflected by increased AMPK phosphorylation and increased substrate metabolism. However, downstream from AMPK, aging-associated pathways such as the mTOR pathway or mitochondrial biogenesis were not affected. Unexpectedly, mild mitochondrial uncoupling in skeletal muscle did not reduce protein oxidative modification in UCP1 TG mice; in contrast, it increased lipid peroxidation-derived modification and led to an induction of several ROS-induced signaling pathways such as increased antioxidant enzyme activity, HSP25, and MAPK signaling.

UCP1 Tg mice show a 40% increased median survival on a high-fat diet and an overall 10% increased lifespan compared with WT mice (30). The data presented here demonstrate that UCP1 Tg mice in younger age are protected from diet-induced obesity despite a higher weight-specific food intake compared with WT mice. However, in a previous study, we could show that they developed obesity comparable with WT littermates in older age while exhibiting an obesity-independent increased insulin sensitivity (30). The molecular mechanisms of the beneficial effect on health and lifespan of mice with skeletal muscle uncoupling are not yet clear. Diet-induced changes in UCP1 content in skeletal muscle of UCP1 Tg mice could be responsible for the lean phenotype. Several authors have proposed that UCP1 content in brown adipose tissue increases after high-fat diet feeding (reviewed in Ref. 14). Here, we show that the ectopically expressed UCP1 protein content in skeletal muscle was not influenced by the diet. To exclude a compensatory effect, we analyzed the expression of UCP3, the main uncoupling protein in skeletal muscle. We did not detect any genotype differences in UCP3 expression of low-fat diet-fed mice. However, UCP3 expression in skeletal muscle was increased in WT mice on a high-fat diet. This is in agreement with prior studies showing an upregulation of UCP3 in skeletal muscle after high-fat diet feeding (13, 31). Our data suggest that an increase in UCP3 is not caused primarily by high-fat diet feeding (no induction of UCP3 in high-fat diet-fed UCP1 Tg mice) but rather linked to body fat accumulation and triglyceride content in muscle, both of which were elevated in high-fat diet-fed WT mice.

Mechanistically, there are several pathways postulated to play a role in longevity, and one important factor is AMPK. Especially in skeletal muscle under conditions of energy demand, for example, during exercise or fasting, AMPK seems to play an important role. Several studies have revealed a decline in responsiveness of AMPK activation in skeletal muscle dur-

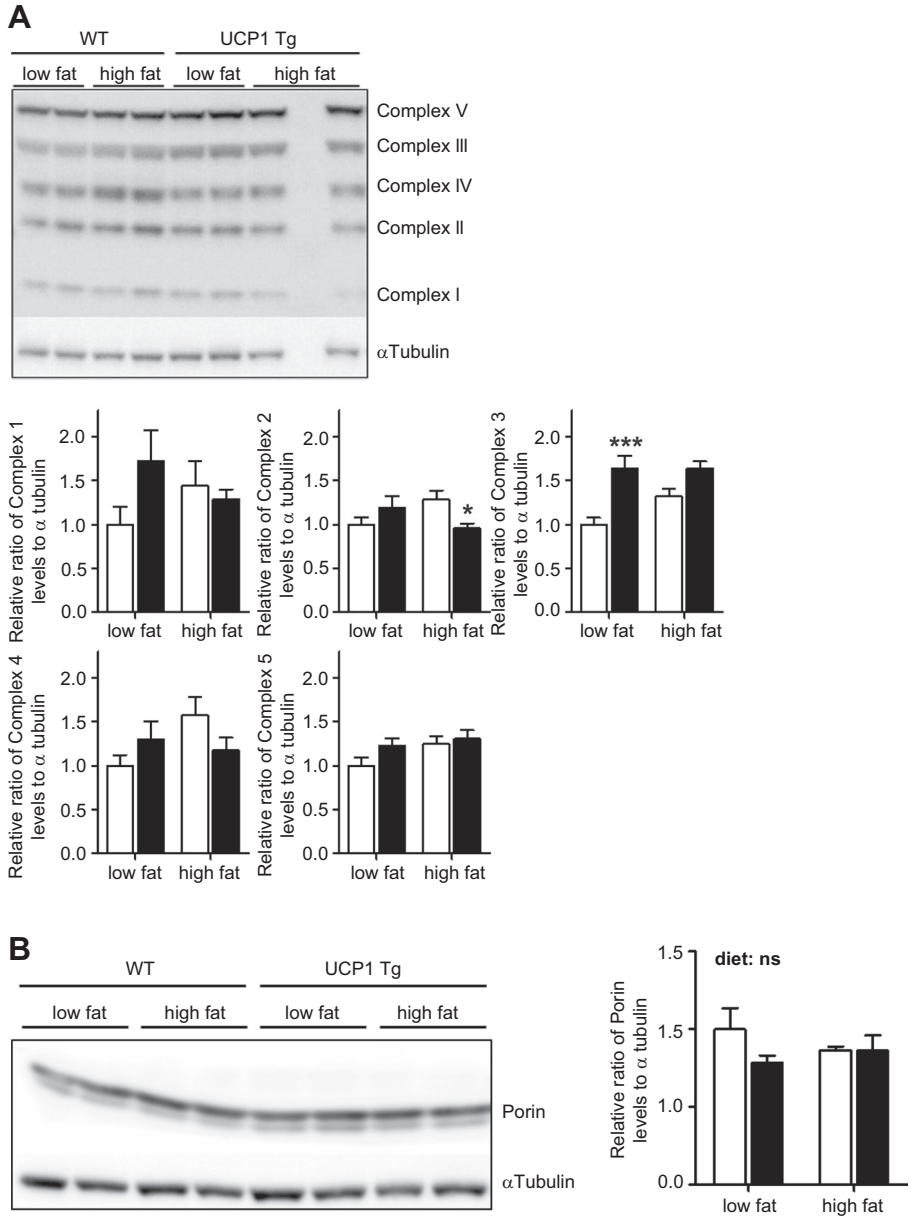

Fig. 4. Mitochondrial biogenesis in skeletal muscle. *A*: Western blot analyses of skeletal muscle protein levels of the complexes of the respiratory chain and the relative ratio of the respiratory chain complexes to α-tubulin of WT (open bars) and UCP1 Tg mice (filled bars) fed a low-fat or high-fat diet. *B*: porin/VDAC in WT and UCP1 Tg mice fed a low-fat or high-fat diet. $*P < 0.05$ and $***P < 0.0001$, significant differences between the genotypes within 1 diet (data are shown as means ± SE relative to the WT low-fat group; $n = 7$).

ing aging (44, 46) and an involvement of AMPK in the regulation of aging processes (reviewed in Ref. 52). Here, we could show an increased phosphorylation of AMPK in UCP1 Tg mice, confirming previous data (17, 38). In skeletal muscle, an organ that plays an important role in insulin sensitivity, activation of AMPK promotes glucose uptake and fatty acid oxidation. Neschen et al. (38) have already shown an increased AMPK phosphorylation and a significantly increased glucose uptake in skeletal muscle of UCP1 Tg animals. In the present study, we focused on lipid metabolism of UCP1 Tg animals, which was also found to be increased. AMPK phosphorylates and thereby inactivates ACC, which decreases malonyl-CoA and hence, abolishes the suppression of fatty acid oxidation in skeletal muscle (63). Phosphorylated ACC was increased in quadriceps muscle of Tg animals compared with WT. Also, the protein expression of fatty acid transporter FAT/CD36, which plays an important role in skeletal muscle fatty acid uptake (5), was increased significantly in Tg mice. Moreover, Bartelt et al. (3) showed recently that FAT/CD36 is one of the major regulators of fatty acid uptake into brown adipose tissue under cold stimulation (when UCP1 is active). Besides protein expression analyses, we could show an overall increased basal fatty acid oxidation in isolated fast-twitch glycolytic EDL as well as the slow-twitch oxidative soleus muscle of UCP1 Tg mice.

AMPK has also been shown to regulate energy metabolism by modulating the activity of the histone/protein deacetylase SIRT1 (8), an enzyme involved in gene expression changes mediating the increase in longevity induced by caloric restriction (49). In another mouse model expressing UCP1 ectopically in skeletal muscle, Gates et al. (17) were able to show a significantly increased SIRT1 activity in muscle, which was more pronounced in aged mice. This is in line with an increased gene expression of SIRT1 in SM of UCP1 Tg mice on

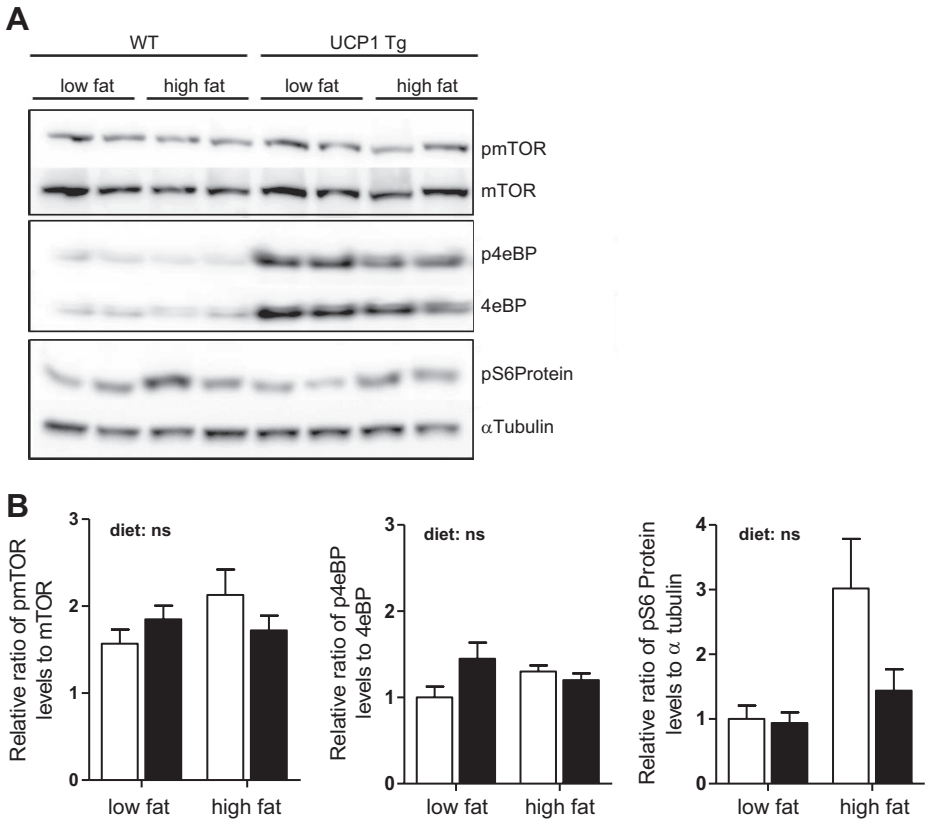

Fig. 5. Mammalian target of rapamycin (mTOR) signaling in skeletal muscle. *A*: Western blot analyses of skeletal muscle protein levels of p-mTOR, mTOR, p-4E-BP, and p-S6 protein. *B*: relative ratio of p-mTOR to mTOR, p-4E-BP to 4E-BP, and p-S6 protein to α-tubulin of WT (open bars) and UCP1 Tg mice (filled bars) fed a low-fat or high-fat diet (data are shown as means ± SE relative to the WT low fat group; $n = 7$).

a low-fat diet in the present study. Surprisingly, and in contrast to the study of Gates et al. (17), we did not detect any effects on the mTOR pathway, which is inhibited by AMPK and is postulated to play an important role in longevity (57). Selman et al. (55) showed that the knockout of the S6 kinase, a downstream target of mTORC1, resulted in an extended lifespan as well as increased insulin sensitivity in mice. Nevertheless, here we could not detect any significant genotype differences in phosphorylation ratio of mTOR or 4E-BP and pS6 protein, suggesting that this mechanism is in our case not involved in the increased longevity of UCP1 Tg mice. However, the total amount of 4E-BP and p-4E-BP protein was increased in UCP1 Tg mice. Phosphorylation of 4E-BP leads to its dissociation from eIF4E, a key rate-limiting initiation factor for translation (18). Recently, the mTOR independent interaction of 4E-BP with the ERK/MAPK signaling pathway, which is differentially regulated in our mouse model, was discussed intensively (11, 37).

Several lines of evidence have suggested a role of oxidative stress in longevity. Thus, the health effects of UCP1 Tg mice could possibly be attributed to the increased mitochondrial uncoupling itself. This would be consistent with the work of

Table 2. *Markers of oxidative, glycoxidative, or lipoxidative stress in skeletal muscle*

	Low Fat		High Fat		ANOVA	
	WT	UCP1 Tg	WT	UCP1 Tg	Diet	Genotype
Muscle, mmol/mol lysine						
MDA	0.23 ± 0.03	0.46 ± 0.10*	0.35 ± 0.04	0.75 ± 0.20*	<0.05	<0.01
CML	0.87 ± 0.16	0.95 ± 0.11	1.29 ± 0.11	1.06 ± 0.15	<0.05	NS
CEL	0.19 ± 0.05	0.21 ± 0.04	0.21 ± 0.02	0.41 ± 0.02	NS	NS
GSA	4.73 ± 0.42	5.40 ± 0.53	5.62 ± 0.31	4.97 ± 0.22	NS	NS
AASA	0.10 ± 0.01	0.20 ± 0.06	015 ± 0.02	0.17 ± 0.04	NS	NS
Aconitase, mU/mg	6.4 ± 0.6	13.5 ± 1.4**	11.8 ± 1.9	19.1 ± 2.3**	<0.001	<0.001
Liver, mmol/mol lysine						
MDA	0.39 ± 0.03	0.25 ± 0.02**	0.77 ± 0.06	0.34 ± 0.05***	<0.0001	<0.0001
CML	1.49 ± 0.15	1.39 ± 0.09	1.54 ± 0.07	1.32 ± 0.07*	NS	NS
CEL	0.37 ± 0.04	0.31 ± 0.05	0.35 ± 0.02	0.34 ± 0.02	NS	NS
GSA	4.86 ± 0.16	4.46 ± 0.19	3.94 ± 0.17	3.72 ± 0.16	<0.001	NS
AASA	0.15 ± 0.02	0.10 ± 0.01	0.15 ± 0.02	0.12 ± 0.02	NS	NS
Aconitase, mU/mg	11.9 ± 0.3	13.2 ± 0.8	10.3 ± 0.2	11.1 ± 0.6	NS	NS

Data are shown as means ± SE; $n = 5–8$. Ne-(malondialdehyde)lysine (MDA), Ne-(carboxymethyl)lysine (CML), Ne-(carboxyethyl)-lysine (CEL), glutamic semialdehyde (GSA), and aminoadipic semialdehyde (AASA) and aconitase in skeletal muscle and liver protein of WT and UCP1 Tg mice fed a low-fat or high-fat diet for 8 wk. *$P < 0.05$, *$P < 0.01$, ***$P < 0.0001$, significant differences between the genotypes within 1 diet group.

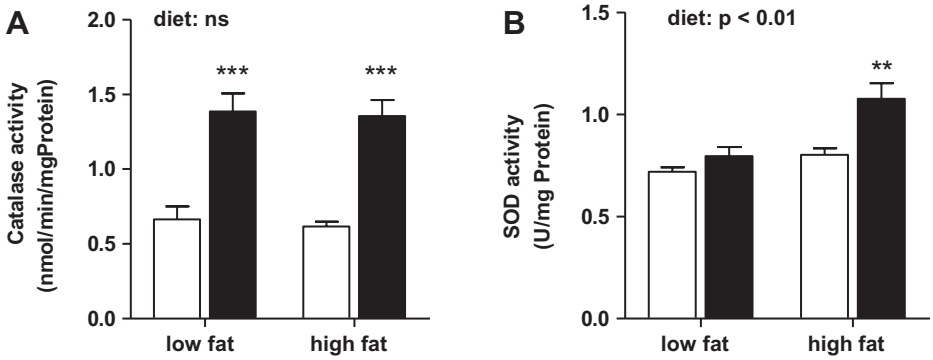

Fig. 6. Antioxidant enzyme activity in skeletal muscle. Enzyme activity of catalase (*A*) and superoxide dismutase (SOD; *B*) of WT (open bars) and UCP1 Tg mice (filled bars) fed a low-fat or high-fat diet. $^{**}P < 0.01$ and $^{***}P < 0.0001$, significant differences between the genotypes within 1 diet group (data are shown as means ± SE relative to the WT low-fat group; $n = 7$).

Speakman et al. (58), who analyzed the relationship between metabolism and lifespan within one species and were able to show that individual mice with high metabolic rates survived the longest. In line with this findings is the "uncoupling to survive" hypothesis, which suggests that increased mitochondrial uncoupling increases longevity by preventing the formation of ROS (6). In a previous study, we could indeed show an ~76% lower superoxide production in isolated SM mitochondria of UCP1 Tg mice that was abolished by the addition of GDP, an inhibitor of UCP1 uncoupling activity (29). Recently, a study by Oelkrug et al. (40) on isolated brown adipose tissue mitochondria of UCP1-knockout mice compared with WT littermates showed that UCP1 decreased superoxide production in brown adipose tissue. They concluded that UCP1 allows high rates of oxidative phosphorylation without enhancing oxidative damage by simultaneously lowering superoxide production. These findings suggested a role of UCPs in keeping superoxide production low by causing mild uncoupling. However, we found no differences in levels of oxidation or glycoxidation markers for protein damage in either skeletal muscle or liver of UCP1 Tg mice. Unexpectedly, UCP1 Tg animals on both diets even showed increased SM protein damage due to lipoxidation-derived reactions compared with WT mice. In contrast to our initial hypothesis, this is indicative of an increased rather than decreased ROS production in skeletal muscle of UCP1 Tg mice. MDA is a specific adduct derived from the nonenzymatic reaction between malondialdehyde (a reactive carbonyl species derived from the oxidative damage of polyunsaturated fatty acids) and free ϵ-amino groups. The increased levels of MDA detected in UCP1 Tg animals could be due to increased ROS production and/or increased content of polyunsaturated fatty acids. So far, no information about the effects of the UCP1 overexpression on membrane fatty acid composition and the potential modulation by the diet is available. However, it is conceivable that UCP1 overexpression in skeletal muscle induces an increase in polyunsaturated fatty acid content, which causes the increase in reactive carbonyl content. This could lead to an increase in lipoxidation-derived protein damage as well as an activation of the antioxidant signaling systems. This is in line with the observation that SM lipids from UCP3-overexpressing mice showed a 20% increment of peroxidizability index, which was due mainly to a 50% increase in the content of the most easily peroxidizable docosahexaenoic acid (7).

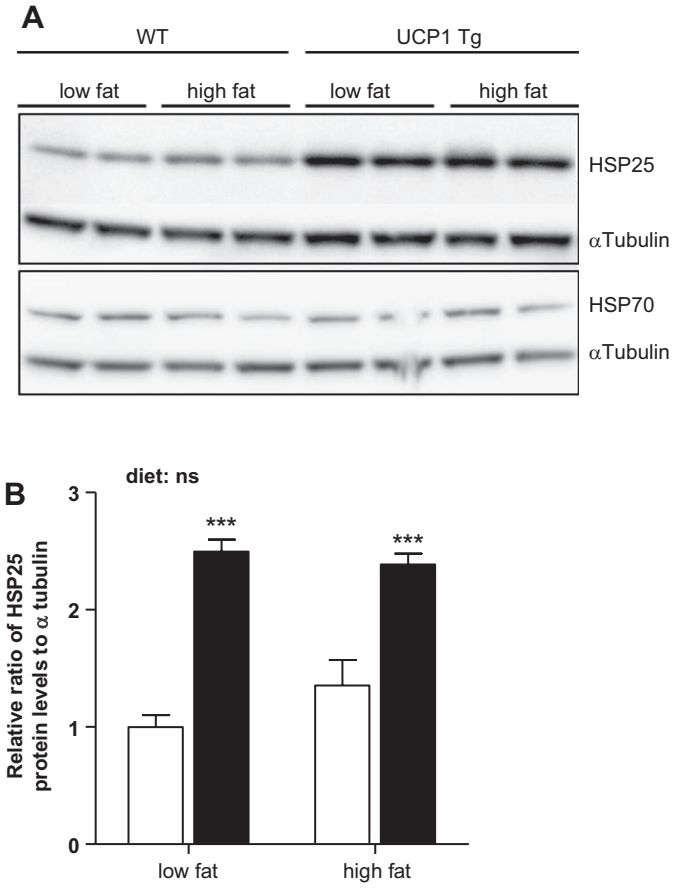

Fig. 7. Heat shock protein (HSP) expression in skeletal muscle. *A*: Western blot analyses of skeletal muscle protein levels. *B*: relative ratio of HSP25 to α-tubulin of WT (open bars) and UCP1 Tg mice (filled bars) fed a low-fat or high-fat diet. $^{***}P < 0.0001$, significant differences between the genotypes within 1 diet group (data are shown as means ± SE relative to the WT low-fat group; $n = 7$).

It is quite difficult to directly measure superoxide production or free radicals in the body. Thus here we focused on endogenous antioxidants and redox signaling pathways to clarify in more detail the oxidative stress status of the muscle cell. The activity of the two antioxidant enzymes SOD and CAT was increased significantly in SM of UCP1 Tg mice compared with WT, especially on the high-fat diet, which suggests a higher stress level in muscle of UCP1 Tg mice. The highly increased CAT activity in UCP1 Tg mice could be linked to their increased longevity. Overexpression of CAT targeted to mitochondria in mice increased median and maximum lifespan by an average of 5 and 5.5 mo, respectively (54), and prevented

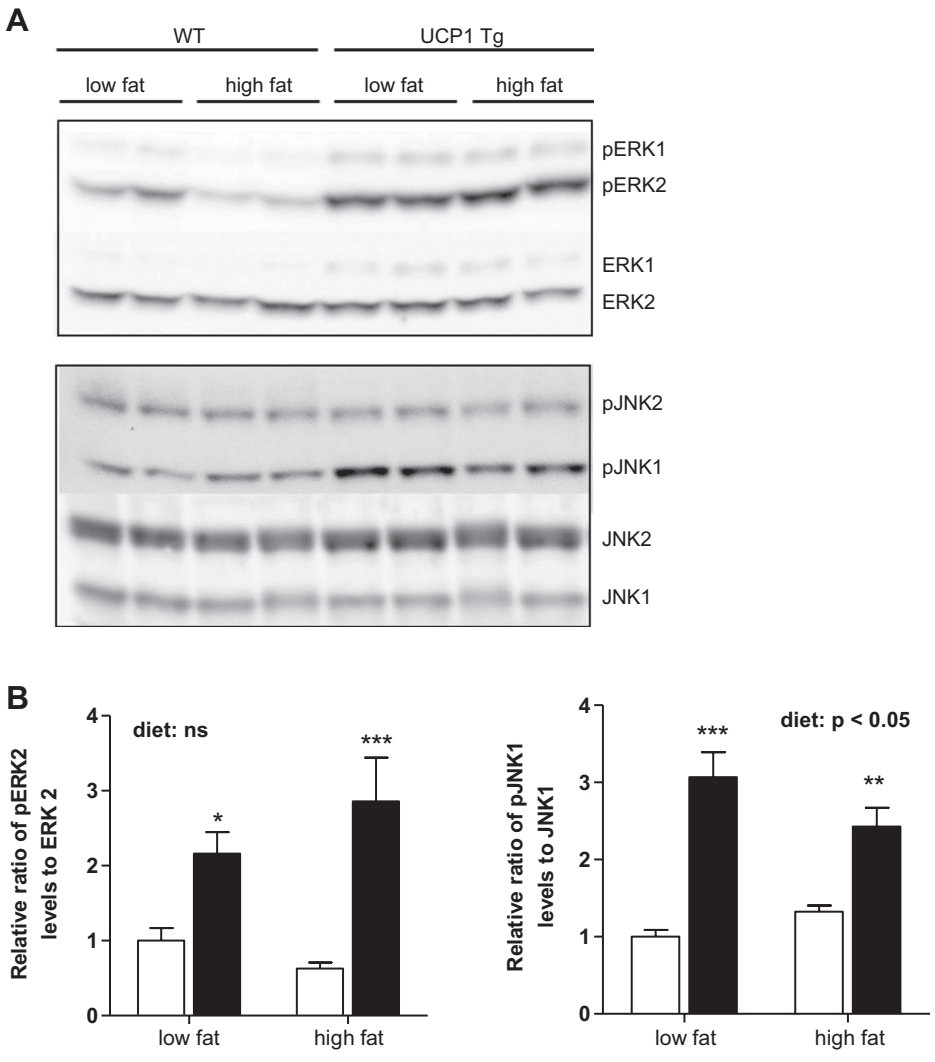

Fig. 8. MAPK signaling in skeletal muscle. Western blot analyses of skeletal muscle protein levels and relative ratio of p-ERK1/2 to ERK1/2 and phosphorylated stress-activated protein kinase (p-SAPK)/JNK1/2 to SAPK/JNK1/2 of WT (open bars) and UCP1 TG mice (filled bars) fed a low-fat or high-fat diet. $*P < 0.05$, $**P < 0.001$, and $***P < 0.0001$, significant differences between the genotypes within 1 diet group (data are shown as means ± SE relative to the WT low fat group; $n = 7$).

age-associated reductions in mitochondrial function and insulin resistance (33).

Another indication for an increased stress situation in SM of UCP1 Tg mice is the strong increase in stress-protective HSP25 protein expression. HSPs act as molecular chaperones, and the expression can increase in response to physical and chemical stressors as well as oxidative stress. Several laboratories (21, 35) have demonstrated that induction of HSPs by heat treatment can protect against obesity-related insulin resistance and that an increased expression of HSP70 and HSP25 plays a significant role in protecting SM from the development of age-related insulin resistance (20). Moreover, the small HSPs especially protect against ROS and stress situations such as ATP depletion (1). Here, we could detect an increased protein content of HSP25 but not of HSP70. One possible explanation is that HSP25 is ATP independent (26), whereas the function of HSP70 is regulated by binding and hydrolysis of ATP (64) and thus dependent on ATPase cycling. Nevertheless, it is yet unresolved whether ATP depletion, heat stress due to UCP1 activity in the SM, or oxidative stress is the trigger for HSP25 upregulation in UCP1 Tg mice.

Another oxidant-induced intracellular signaling cascade is the MAPK pathway, which plays an essential role for the induction of oxidative stress response (reviewed in Ref. 50). ROS and other reactive species are potential activators of ERK1/2 and JNK1/2 (34). Furthermore, it is well known that exercise, itself an intermittent form of cellular stress, activates the MAPK signaling pathway in skeletal muscle of mice (19, 36) and humans (62), depending on the type, duration, and intensity of the muscle work. UCP1 Tg mice showed a more than twofold increase in phosphorylated ERK2 and phosphorylated JNK1. The activity of ERK1/2 is associated with various aspects of lipid metabolism. It seems to be involved in the phosphorylation of ACC and hormone-sensitive lipase (12) as well as fatty acid uptake during muscle activity (45, 59). Therefore, the increased ERK2 in UCP1 Tg mice could explain their increased SM fatty acid metabolism. Not only ERK2 but also the JNK1 was highly phosphorylated in our Tg mouse model. The stress-activated kinase JNK plays on the one hand a critical role in stress induced cell death but on the other hand also has a protective function in response to oxidative stress and has been implicated in the regulation of lifespan (reviewed in Ref. 27). Nevertheless, JNK1 is elevated in obesity, and furthermore, the inhibition of JNK activity improved insulin sensitivity in mice and protected them from diet-induced obesity (24). This is in agreement with our observation that WT

mice on a high-fat diet showed a significantly increased JNK1 phosphorylation compared with WT mice on a low-fat diet. However, recently, Sharma et al. (56) showed that caloric restriction led to an increased JNK1 phosphorylation in rats despite improved insulin sensitivity. Thus, whether JNK signaling is protective of or detrimental to the muscle cell remains incompletely understood and is probably dependent on the duration and/or intensity of its activation.

Nevertheless, our data regarding the oxidative stress status of SM support the notion of an increased rather than decreased radical production in SM of UCP1 Tg mice. An imbalance in the oxidative stress status, which leads to elevated ROS levels, acts as a trigger for insulin resistance (25). However, UCP1 Tg mice have shown increased insulin sensitivity and increased lifespan compared with WT mice under detrimental dietary conditions (30). The data of this study are in agreement with the concept of mitohormesis, which suggests that mild oxidative stress is required to prolong lifespan (47). An increased formation of ROS might cause an adaptive response by increasing oxidative defense, which ultimately leads to reduced oxidative stress damage. This is in line with the increased antioxidant enzyme activities and the higher aconitase activity in SM of UCP1 Tg mice compared with WT presented here. Aconitase activity is a sensitive marker of superoxide concentration because superoxide inactivates aconitase in the mitochondrial matrix (16). Especially in skeletal muscle during contraction and physical exercise, oxygen consumption increases dramatically, which leads to a corresponding increase in free radical production paralleled by an induction of the expression of antioxidants (22, 43). Ristow et al. (48) were able to show that the exercise-induced free radical production leads to an increased expression of endogenous antioxidants and promotes insulin sensitivity in humans rather than inducing insulin resistance. Recently, Boden et al. (4) demonstrated that overexpression of the antioxidant manganese superoxide dismutase in rat skeletal muscle in vivo partially protects the muscle against impaired glucose uptake under high-fat diet conditions. Thus, the induction of endogenous antioxidants may contribute to the protection against diet-induced insulin resistance in SM of UCP1 Tg mice.

In conclusion, our results show that SM uncoupling leads to an energy demand in the muscle cell, which results in the activation of AMPK but also in a mild stress induction that in turn increases endogenous antioxidant defense systems. The activation of AMPK is accompanied by an increased lipid metabolism but not by a downregulation of the mTOR pathway. Therefore, we suggest that the increased longevity phenotype of UCP1 Tg mice on a high-fat diet is rather linked to the induction of ROS-signaling pathways. This argues for the hypothesis that ROS and perhaps lipid-derived carbonyl species are not only damaging agents but important physiological signaling molecules.

ACKNOWLEDGMENTS

We thank Antje Sylvester for technical assistance.

GRANTS

The research leading to these results has received funding from the European Union's Seventh Framework Program FP7 2007–2013 under grant agreement no. 244995 (BIOCLAIMS Project) and from the German Research Foundation (DFG: KL613/14-2). The studies conducted at the Department of Experimental Medicine were supported in part by research and development grants from the Spanish Ministry of Science and Innovation (BFU2009–11879/BFI), the Spanish Ministry of Health (PI08111532), the Autonomous Government of Catalonia (2009SGR735), and COST B35 Action of the European Union.

DISCLOSURES

The authors have nothing to declare and no conflicts of interest to disclose, financial or otherwise.

AUTHOR CONTRIBUTIONS

S. Keipert, M.O., A.C., A.V., and V.A. performed the experiments; S. Keipert, A.C., V.A., and R.P. analyzed the data; S. Keipert, A.C., M.P.-O., R.P., and H.A.-H. interpreted the results of the experiments; S. Keipert prepared the figures; S. Keipert drafted the manuscript; M.O., A.V., M.P.-O., R.P., H.A.-H., and S. Klaus edited and revised the manuscript; S. Klaus contributed to the conception and design of the research; S. Klaus approved the final version of the manuscript.

REFERENCES

1. **Arrigo AP.** The cellular "networking" of mammalian Hsp27 and its functions in the control of protein folding, redox state and apoptosis. *Adv Exp Med Biol* 594: 14–26, 2007.
2. **Barnes BR, Marklund S, Steiler TL, Walter M, Hjalm G, Amarger V, Mahlapuu M, Leng Y, Johansson C, Galuska D, Lindgren K, Abrink M, Stapleton D, Zierath JR, Andersson L.** The 5′-AMP-activated protein kinase gamma3 isoform has a key role in carbohydrate and lipid metabolism in glycolytic skeletal muscle. *J Biol Chem* 279: 38441–38447, 2004.
3. **Bartelt A, Bruns OT, Reimer R, Hohenberg H, Ittrich H, Peldschus K, Kaul MG, Tromsdorf UI, Weller H, Waurisch C, Eychmuller A, Gordts PL, Rinninger F, Bruegelmann K, Freund B, Nielsen P, Merkel M, Heeren J.** Brown adipose tissue activity controls triglyceride clearance. *Nat Med* 17: 200–205, 2011.
4. **Boden MJ, Brandon AE, Tid-Ang JD, Preston E, Wilks D, Stuart E, Cleasby ME, Turner N, Cooney GJ, Kraegen EW.** Overexpression of manganese superoxide dismutase ameliorates high-fat diet-induced insulin resistance in rat skeletal muscle. *Am J Physiol Endocrinol Metab* 303: E798–E805, 2012.
5. **Bonen A, Han XX, Habets DD, Febbraio M, Glatz JF, Luiken JJ.** A null mutation in skeletal muscle FAT/CD36 reveals its essential role in insulin- and AICAR-stimulated fatty acid metabolism. *Am J Physiol Endocrinol Metab* 292: E1740–E1749, 2007.
6. **Brand MD.** Uncoupling to survive? The role of mitochondrial inefficiency in ageing. *Exp Gerontol* 35: 811–820, 2000.
7. **Brand MD, Pamplona R, Portero-Otin M, Requena JR, Roebuck SJ, Buckingham JA, Clapham JC, Cadenas S.** Oxidative damage and phospholipid fatty acyl composition in skeletal muscle mitochondria from mice underexpressing or overexpressing uncoupling protein 3. *Biochem J* 368: 597–603, 2002.
8. **Canto C, Gerhart-Hines Z, Feige JN, Lagouge M, Noriega L, Milne JC, Elliott PJ, Puigserver P, Auwerx J.** AMPK regulates energy expenditure by modulating NAD+ metabolism and SIRT1 activity. *Nature* 458: 1056–1060, 2009.
9. **Chadt A, Leicht K, Deshmukh A, Jiang LQ, Scherneck S, Bernhardt U, Dreja T, Vogel H, Schmolz K, Kluge R, Zierath JR, Hultschig C, Hoeben RC, Schürmann A, Joost HG, Al-Hasani H.** Tbc1d1 mutation in lean mouse strain confers leanness and protects from diet-induced obesity. *Nat Genet* 40: 1354–1359, 2008.
10. **Chomczynski P, Sacchi N.** Single-step method of RNA isolation by acid guanidinium thiocyanate-phenol-chloroform extraction. *Anal Biochem* 162: 156–159, 1987.
11. **Cohen JD, Gard JM, Nagle RB, Dietrich JD, Monks TJ, Lau SS.** ERK crosstalks with 4eBP1 to activate cyclin D1 translation during quinol-thioether-induced tuberous sclerosis renal cell carcinoma. *Toxicol Sci* 124: 75–87, 2011.
12. **Donsmark M, Langfort J, Holm C, Ploug T, Galbo H.** Contractions activate hormone-sensitive lipase in rat muscle by protein kinase C and mitogen-activated protein kinase. *J Physiol* 550: 845–854, 2003.
13. **Felipe F, Bonet ML, Ribot J, Palou A.** Up-regulation of muscle uncoupling protein 3 gene expression in mice following high fat diet, dietary

vitamin A supplementation and acute retinoic acid-treatment. *Int J Obes Relat Metab Disord* 27: 60–69, 2003.
14. **Fromme T, Klingenspor M.** Uncoupling protein 1 expression and high-fat diets. *Am J Physiol Regul Integr Comp Physiol* 300: R1–R8, 2011.
15. **Furukawa S, Fujita T, Shimabukuro M, Iwaki M, Yamada Y, Nakajima Y, Nakayama O, Makishima M, Matsuda M, Shimomura I.** Increased oxidative stress in obesity and its impact on metabolic syndrome. *J Clin Invest* 114: 1752–1761, 2004.
16. **Gardner PR.** Aconitase: sensitive target and measure of superoxide. *Methods Enzymol* 349: 9–23, 2002.
17. **Gates AC, Bernal-Mizrachi C, Chinault SL, Feng C, Schneider JG, Coleman T, Malone JP, Townsend RR, Chakravarthy MV, Semenkovich CF.** Respiratory uncoupling in skeletal muscle delays death and diminishes age-related disease. *Cell Metab* 6: 497–505, 2007.
18. **Gingras AC, Raught B, Gygi SP, Niedzwiecka A, Miron M, Burley SK, Polakiewicz RD, Wyslouch-Cieszynska A, Aebersold R, Sonenberg N.** Hierarchical phosphorylation of the translation inhibitor 4E-BP1. *Genes Dev* 15: 2852–2864, 2001.
19. **Goodyear LJ, Chang PY, Sherwood DJ, Dufresne SD, Moller DE.** Effects of exercise and insulin on mitogen-activated protein kinase signaling pathways in rat skeletal muscle. *Am J Physiol Endocrinol Metab* 271: E403–E408, 1996.
20. **Gupte AA, Bomhoff GL, Geiger PC.** Age-related differences in skeletal muscle insulin signaling: the role of stress kinases and heat shock proteins. *J Appl Physiol* 105: 839–848, 2008.
21. **Gupte AA, Bomhoff GL, Swerdlow RH, Geiger PC.** Heat treatment improves glucose tolerance and prevents skeletal muscle insulin resistance in rats fed a high-fat diet. *Diabetes* 58: 567–578, 2009.
22. **Higashida K, Kim SH, Higuchi M, Holloszy JO, Han DH.** Normal adaptations to exercise despite protection against oxidative stress. *Am J Physiol Endocrinol Metab* 301: E779–E784, 2011.
23. **Hiona A, Sanz A, Kujoth GC, Pamplona R, Seo AY, Hofer T, Someya S, Miyakawa T, Nakayama C, Samhan-Arias AK, Servais S, Barger JL, Portero-Otin M, Tanokura M, Prolla TA, Leeuwenburgh C.** Mitochondrial DNA mutations induce mitochondrial dysfunction, apoptosis and sarcopenia in skeletal muscle of mitochondrial DNA mutator mice. *PLoS One* 5: e11468, 2010.
24. **Hirosumi J, Tuncman G, Chang L, Gorgun CZ, Uysal KT, Maeda K, Karin M, Hotamisligil GS.** A central role for JNK in obesity and insulin resistance. *Nature* 420: 333–336, 2002.
25. **Houstis N, Rosen ED, Lander ES.** Reactive oxygen species have a causal role in multiple forms of insulin resistance. *Nature* 440: 944–948, 2006.
26. **Jakob U, Gaestel M, Engel K, Buchner J.** Small heat shock proteins are molecular chaperones. *J Biol Chem* 268: 1517–1520, 1993.
27. **Karpac J, Jasper H.** Insulin and JNK: optimizing metabolic homeostasis and lifespan. *Trends Endocrinol Metab* 20: 100–106, 2009.
28. **Katterle Y, Keipert S, Hof J, Klaus S.** Dissociation of obesity and insulin resistance in transgenic mice with skeletal muscle expression of uncoupling protein 1. *Physiol Genomics* 32: 352–359, 2008.
29. **Keipert S, Klaus S, Heldmaier G, Jastroch M.** UCP1 ectopically expressed in murine muscle displays native function and mitigates mitochondrial superoxide production. *Biochim Biophys Acta* 1797: 324–330, 2010.
30. **Keipert S, Voigt A, Klaus S.** Dietary effects on body composition, glucose metabolism, and longevity are modulated by skeletal muscle mitochondrial uncoupling in mice. *Aging Cell* 10: 122–136, 2011.
31. **Khalfallah Y, Fages S, Laville M, Langin D, Vidal H.** Regulation of uncoupling protein-2 and uncoupling protein-3 mRNA expression during lipid infusion in human skeletal muscle and subcutaneous adipose tissue. *Diabetes* 49: 25–31, 2000.
32. **Klaus S, Rudolph B, Dohrmann C, Wehr R.** Expression of uncoupling protein 1 in skeletal muscle decreases muscle energy efficiency and affects thermoregulation and substrate oxidation. *Physiol Genomics* 21: 193–200, 2005.
33. **Lee HY, Choi CS, Birkenfeld AL, Alves TC, Jornayvaz FR, Jurczak MJ, Zhang D, Woo DK, Shadel GS, Ladiges W, Rabinovitch PS, Santos JH, Petersen KF, Samuel VT, Shulman GI.** Targeted expression of catalase to mitochondria prevents age-associated reductions in mitochondrial function and insulin resistance. *Cell Metab* 12: 668–674, 2010.
34. **McCubrey JA, Lahair MM, Franklin RA.** Reactive oxygen species-induced activation of the MAP kinase signaling pathways. *Antioxid Redox Signal* 8: 1775–1789, 2006.
35. **Morino S, Kondo T, Sasaki K, Adachi H, Suico MA, Sekimoto E, Matsuda T, Shuto T, Araki E, Kai H.** Mild electrical stimulation with heat shock ameliorates insulin resistance via enhanced insulin signaling. *PLoS One* 3: e4068, 2008.
36. **Nader GA, Esser KA.** Intracellular signaling specificity in skeletal muscle in response to different modes of exercise. *J Appl Physiol* 90: 1936–1942, 2001.
37. **Nawroth R, Stellwagen F, Schulz WA, Stoehr R, Hartmann A, Krause BJ, Gschwend JE, Retz M.** S6K1 and 4E-BP1 are independent regulated and control cellular growth in bladder cancer. *PLoS One* 6: e27509, 2011.
38. **Neschen S, Katterle Y, Richter J, Augustin R, Scherneck S, Mirhashemi F, Schurmann A, Joost HG, Klaus S.** Uncoupling protein 1 expression in murine skeletal muscle increases AMPK activation, glucose turnover, and insulin sensitivity in vivo. *Physiol Genomics* 33: 333–340, 2008.
39. **Noatsch A, Petzke KJ, Millrose MK, Klaus S.** Body weight and energy homeostasis was not affected in C57BL/6 mice fed high whey protein or leucine-supplemented low-fat diets. *Eur J Nutr* 50: 479–488, 2010.
40. **Oelkrug R, Kutschke M, Meyer CW, Heldmaier G, Jastroch M.** Uncoupling protein 1 decreases superoxide production in brown adipose tissue mitochondria. *J Biol Chem* 285: 21961–21968, 2010.
41. **Pamplona R, Barja G.** Mitochondrial oxidative stress, aging and caloric restriction: the protein and methionine connection. *Biochim Biophys Acta* 1757: 496–508, 2006.
42. **Portero-Otin M, Requena JR, Bellmunt MJ, Ayala V, Pamplona R.** Protein nonenzymatic modifications and proteasome activity in skeletal muscle from the short-lived rat and long-lived pigeon. *Exp Gerontol* 39: 1527–1535, 2004.
43. **Powers SK, Jackson MJ.** Exercise-induced oxidative stress: cellular mechanisms and impact on muscle force production. *Physiol Rev* 88: 1243–1276, 2008.
44. **Qiang W, Weiqiang K, Qing Z, Pengju Z, Yi L.** Aging impairs insulin-stimulated glucose uptake in rat skeletal muscle via suppressing AMPKalpha. *Exp Mol Med* 39: 535–543, 2007.
45. **Raney MA, Turcotte LP.** Regulation of contraction-induced FA uptake and oxidation by AMPK and ERK1/2 is intensity dependent in rodent muscle. *Am J Physiol Endocrinol Metab* 291: E1220–E1227, 2006.
46. **Reznick RM, Zong H, Li J, Morino K, Moore IK, Yu HJ, Liu ZX, Dong J, Mustard KJ, Hawley SA, Befroy D, Pypaert M, Hardie DG, Young LH, Shulman GI.** Aging-associated reductions in AMP-activated protein kinase activity and mitochondrial biogenesis. *Cell Metab* 5: 151–156, 2007.
47. **Ristow M, Zarse K.** How increased oxidative stress promotes longevity and metabolic health: The concept of mitochondrial hormesis (mitohormesis). *Exp Gerontol* 45: 410–418, 2010.
48. **Ristow M, Zarse K, Oberbach A, Kloting N, Birringer M, Kiehntopf M, Stumvoll M, Kahn CR, Bluher M.** Antioxidants prevent health-promoting effects of physical exercise in humans. *Proc Natl Acad Sci USA* 106: 8665–8670, 2009.
49. **Ruderman NB, Xu XJ, Nelson L, Cacicedo JM, Saha AK, Lan F, Ido Y.** AMPK and SIRT1: a long-standing partnership? *Am J Physiol Endocrinol Metab* 298: E751–E760, 2010.
50. **Runchel C, Matsuzawa A, Ichijo H.** Mitogen-activated protein kinases in mammalian oxidative stress responses. *Antioxid Redox Signal* 15: 205–218, 2011.
51. **Rustin P, Chretien D, Bourgeron T, Gerard B, Rotig A, Saudubray JM, Munnich A.** Biochemical and molecular investigations in respiratory chain deficiencies. *Clin Chim Acta* 228: 35–51, 1994.
52. **Salminen A, Kaarniranta K.** AMP-activated protein kinase (AMPK) controls the aging process via an integrated signaling network. *Ageing Res Rev* 11: 230–241, 2012.
53. **Sanz A, Pamplona R, Barja G.** Is the mitochondrial free radical theory of aging intact? *Antioxid Redox Signal* 8: 582–599, 2006.
54. **Schriner SE, Linford NJ, Martin GM, Treuting P, Ogburn CE, Emond M, Coskun PE, Ladiges W, Wolf N, Van Remmen H, Wallace DC, Rabinovitch PS.** Extension of murine life span by overexpression of catalase targeted to mitochondria. *Science* 308: 1909–1911, 2005.
55. **Selman C, Tullet JM, Wieser D, Irvine E, Lingard SJ, Choudhury AI, Claret M, Al-Qassab H, Carmignac D, Ramadani F, Woods A, Robinson IC, Schuster E, Batterham RL, Kozma SC, Thomas G, Carling D, Okkenhaug K, Thornton JM, Partridge L, Gems D, Withers DJ.** Ribosomal protein S6 kinase 1 signaling regulates mammalian life span. *Science* 326: 140–144, 2009.
56. **Sharma N, Bhat AD, Kassa AD, Xiao Y, Arias EB, Cartee GD.** Improved insulin sensitivity with calorie restriction does not require reduced JNK1/2,

p38, or ERK1/2 phosphorylation in skeletal muscle of 9-month-old rats. *Am J Physiol Regul Integr Comp Physiol* 302: R126–R136, 2012.
57. **Shaw RJ.** LKB1 and AMP-activated protein kinase control of mTOR signalling and growth. *Acta Physiol (Oxf)* 196: 65–80, 2009.
58. **Speakman JR, Talbot DA, Selman C, Snart S, McLaren JS, Redman P, Krol E, Jackson DM, Johnson MS, Brand MD.** Uncoupled and surviving: individual mice with high metabolism have greater mitochondrial uncoupling and live longer. *Aging Cell* 3: 87–95, 2004.
59. **Turcotte LP, Raney MA, Todd MK.** ERK1/2 inhibition prevents contraction-induced increase in plasma membrane FAT/CD36 content and FA uptake in rodent muscle. *Acta Physiol Scand* 184: 131–139, 2005.
60. **Urakawa H, Katsuki A, Sumida Y, Gabazza EC, Murashima S, Morioka K, Maruyama N, Kitagawa N, Tanaka T, Hori Y, Nakatani K, Yano Y, Adachi Y.** Oxidative stress is associated with adiposity and insulin resistance in men. *J Clin Endocrinol Metab* 88: 4673–4676, 2003.
61. **Weber K, Bolander ME, Sarkar G.** PIG-B: a homemade monophasic cocktail for the extraction of RNA. *Mol Biotechnol* 9: 73–77, 1998.
62. **Widegren U, Wretman C, Lionikas A, Hedin G, Henriksson J.** Influence of exercise intensity on ERK/MAP kinase signalling in human skeletal muscle. *Pflugers Arch* 441: 317–322, 2000.
63. **Winder WW, Wilson HA, Hardie DG, Rasmussen BB, Hutber CA, Call GB, Clayton RD, Conley LM, Yoon S, Zhou B.** Phosphorylation of rat muscle acetyl-CoA carboxylase by AMP-activated protein kinase and protein kinase A. *J Appl Physiol* 82: 219–225, 1997.
64. **Young JC.** Mechanisms of the Hsp70 chaperone system. *Biochem Cell Biol* 88: 291–300, 2010.